Journal of Manufacturing Engineering, December 2021, Vol. 16, Issue. 4, pp 108- 114

DESIGN OF POROUS STEP BEARING BY CONSIDERING DIFFERENT FERRO FLUID LUBRICATION FLOW MODELS

***Dipak A Patel[1], Manisha Joshi[2] and Dilip B Patel[3]**

[1]Humanities and Sciences Department, Government Engineering College Palanpur, Gujarat – 385001, India
[2]Department of Mathematics, IILM University, Gurugram, Haryana – 122003, India
[3]College of Renewable Energy and Environmental Engineering, S. D. Agricultural University, Sardarkrushinagar, Gujarat – 385506, India

ABSTRACT

The aim of this article is to carry out an analysis to enhance the performance of the ferrofluid lubricated porous step bearing. The porous coating is assorted to the lower flat impermeable surface. A step is there in the upper surface, which approaches the lower surface. This study considered that the magnetic field is flexible and oblique to the lower surface. By considering Jenkins Model, expressions for pressure and load capacity are obtained. The non-dimensional load capacity is also calculated for various parameters. Based on the results, it is observed that load capacity increases if a suitable step size is considered. Also, a comparison between R. E. Rosensweig Model and Jenkins Model is carried out. Finally, designing a porous step bearing, one should consider Jenkins Model over R. E. Rosensweig Model.

Keywords: Step bearing, ferrofluid lubrication, R. E. Rosensweig Model and Jenkins Model and Load Capacity

1. Introduction

Step bearings are widely studied since they are used in industry as thrust bearing due to their benefit in machinery load and minimizing cost. To improve the performance of vibrations in rotors, journal bearings also have some steps.

In 1993, Leek et al. [1] studied an electro-rheological fluid flow experimentally in the case of Rayleigh step bearing. Shah [2] studied ferrofluid lubricated step bearing and concluded that by using ferrofluid (FF), one could improve the bearing performance. Later on, in 2014, Shah and Patel [3] analyzed magnetic fluid (MF) lubricated step bearing by considering various porous structures and determined that better load was obtained in the globular sphere model than that of the capillary fissure model. They have considered Neuringer-Rosenweig Model (NR Model) [4] for their study.

Squeeze velocity [5] occurs when lubricated surfaces approach each other in the fluid film region. Such velocity is so-called squeeze velocity. Squeeze film behaviour is observed in numerous applications such as gears, bearings, hydraulic systems, rolling elements, clutch plates, human knee joints, etc.

As exotic magnetic colloids, ferromagnetic ferrofluids have excellent tribological features for several applications in mechanical engineering. The details can be seen in Rosensweig [4].

When external magnetic field B is applied on the film region, the fluids experience magnetic body forces $(M.\nabla)$ B, which depends upon the magnetization vector M due to ferromagnetic particles. These features are helpful in many applications such as sensors, elastic damper, filtering apparatus, bearings, etc. [4-9]. Verma [10] deliberate squeeze film bearing (MF lubricated) using three porous coats attached to the lower surface and exhibited that due to the effect of MF lubricant, load-carrying capacity increases as compared to conventional fluid lubricant. Many researchers (for example, [10-13]) have studied MF lubricated various designed bearings like porous slider bearings, axially undefined journal bearing, squeeze film bearings in the presence of slip velocity and anisotropic permeability.

This study aims to obtain Reynold's type equation for porous step bearing (water-based FF lubricated) by considering Jenkins's Model (JE Model). In the present study, the magnetic field is variable and tilted to the lower plate. Also, non-dimensional load carrying capacity and non-dimensional pressure is calculated by considering suitable boundary conditions for various parameters like the impact of width of the porous layer, step size, permeability, magnetic field strength, and width of the film region.

**Corresponding Author - E- mail: da.ab44@gmail.com*

2. Mathematical Demonstrating of the problem

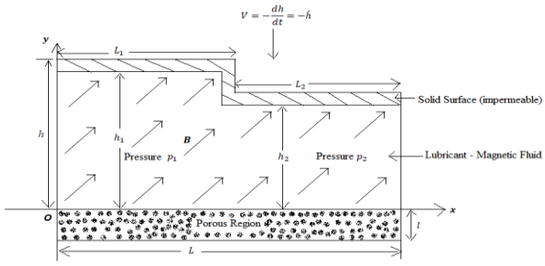

Fig. 1 Step bearing system

Many types of step bearings are used in machinery. Fig. 1 shows the step bearing system having length L in *x*-direction considered for the study. The porous layer is attached to the lower surface having width l. The two plates are separated by MF, which is in the film region in the *y*-direction, having a height h ($h >> L$). The first step has a length L_1 and height $h_1 = h$ and the second step has a length L_2 and height h_2. Also, from the figure, it is clear that $h_1 > h_2$ and the squeeze velocity is $V = -\frac{dh}{dt} = -\dot{h}$. The pressure in the porous region is P whereas in the first and second step the fluid pressure is p_1 and p_2 respectively. The external magnetic field vector is denoted by $\boldsymbol{B}$.

3. Flow Models of Magnetic Fluid Flow

In 1964, Neuringer and Rosensweig [4] proposed a simple model for the flow of magnetic fluids in the presence of fluctuating external magnetic fields. The NR Model's fundamental flow equations are as follows:

$$\rho[\bar{q}.\nabla]\bar{q} = -\nabla p + \eta\nabla^2\bar{q} + \mu_0(\bar{M}.\nabla)\mathbf{B}, \quad (1)$$

$$\nabla.\bar{q} = 0, \quad (2)$$

$$\nabla \times \mathbf{B} = 0, \quad (3)$$

$$\nabla.(\mathbf{B} + \bar{M}) = 0, \quad (4)$$

$$\bar{M} = \bar{\mu}\mathbf{B}, \quad (5)$$

where ρ is the density of fluid, $\bar{q}$ is the fluid velocity vector in film region, p is film pressure,η is the viscosity of fluid, μ_0 is free space permeability, $\bar{M}$ is the magnetization vector, **B** is the applied magnetic field, $\bar{\mu}$ is magnetic susceptibility of the fluid. The details can be seen in [14]. In 1972, Jenkins modified the NR flow Model to describe the flow of MF. By considering Maugin's modification [15, 16], equations of JE model for steady fluid flow are

$$\rho[\bar{q}.\nabla]\bar{q} = -\nabla p + \eta\nabla^2\bar{q} + \mu_0(\bar{M}.\nabla)\mathbf{B} + \rho\alpha^2\nabla \times \left(\frac{\bar{M}}{M} \times \bar{M}^*\right), \quad (6)$$

$$\nabla.(\mathbf{B} + 4\pi\bar{M}) = 0, \quad (7)$$

$$\bar{M} = \bar{\mu}B, \quad (8)$$

and

$$\bar{M}^* = \frac{1}{2}(\nabla \times \bar{q}) \times \bar{M}, \quad (9)$$

In (6), α^2 is the material parameter (the SI unit of α^2 is $m^3s^{-1}A^{-1}$), M is magnetization strength, and B is applied magnetic field strength.

4. Analysis

Using the conventions of hydrodynamic lubrication and the flow is stable and axially symmetrical, (2), (3), (6)-(9) turns out to be

$$\frac{\partial^2 u}{\partial y^2} = \frac{1}{\eta\left(1-\frac{\rho\alpha^2\bar{\mu}B}{2\eta}\right)}\frac{d}{dx}\left(p - \frac{1}{2}\mu_0\bar{\mu}B^2\right), \quad (10)$$

where expression of B is

$$B^2 = Kx(L - x), \quad (11)$$

In (11), K is quantity chosen such that the field strength and the dimensions of both sides of (11) are the same. If φ_x and $\eta_x$denotes the permeability in the lower porous matrix in the *x*-direction and the porosity of the lower porous region in the *x*-direction, respectively, solving (10) under the boundary conditions [11]

$$u = \frac{1}{s}\frac{\partial u}{\partial y}, \ when\ y = 0$$

and $u = 0, when\ y = h,$

where 'h' is film thickness, s is a slip defined by $\frac{1}{s} = \frac{\sqrt{\varphi_x\eta_x}}{5}$, one attains

$$u = \frac{(1+hs)y - syh^2 - h^2}{2\eta(1+hs)\left(1-\frac{\rho\alpha^2\bar{\mu}B}{2\eta}\right)}\frac{\partial}{\partial x}\left(p - \frac{1}{2}\mu_0\bar{\mu}B^2\right) \quad (12)$$

The components of the fluid velocity in the porous region in *x*-direction and y-direction are

$$\bar{u} = -\frac{\varphi_x}{\eta}\left[\frac{\partial}{\partial x}\left(P - \frac{1}{2}\mu_0\bar{\mu}B^2\right) + \frac{\rho\alpha^2\bar{\mu}}{2}\frac{\partial}{\partial y}\left(B\frac{\partial u}{\partial y}\right)\right] \quad (13)$$

and

$$\bar{w} = -\frac{\varphi_y}{\eta}\left[\frac{\partial}{\partial y}\left(P - \frac{1}{2}\mu_0\bar{\mu}B^2\right) - \frac{\rho\alpha^2\bar{\mu}}{2}\frac{\partial}{\partial x}\left(B\frac{\partial u}{\partial y}\right)\right] \quad (14)$$

respectively. In (13) and (14), P denotes fluid pressure in the porous region and φ_y represents permeability in the lower porous matrix in the y-direction. Next, the equation of continuity in the porous matrix is

$$\frac{\partial \bar{u}}{\partial x} + \frac{\partial \bar{w}}{\partial y} = 0. \quad (15)$$

By using (13) & (14) and integrating (15) with respect to y over $(-l, 0)$ yields

$$\varphi_x l\frac{\partial^2}{\partial x^2}\left(P - \frac{1}{2}\mu_0\bar{\mu}B^2\right) + \varphi_y\frac{\partial}{\partial y}\left(P - \frac{1}{2}\mu_0\bar{\mu}B^2\right)\Big|_{y=0} + \left(\varphi_x - \varphi_y\right)\frac{\rho\alpha^2\bar{\mu}}{2}\frac{\partial}{\partial x}\left(B\frac{\partial u}{\partial y}\right)\Big|_{y=-l}^{y=0} = 0 \quad (16)$$

According to Morgan–Cameron approximation [17], the surface is solid at $y = -l$. Equation (16) is equivalent to

$$\frac{\partial}{\partial y}\left(P - \frac{1}{2}\mu_0\bar{\mu}B^2\right)\Big|_{y=0} = -\frac{\varphi_x l}{\varphi_y}\frac{\partial^2}{\partial x^2}\left(P - \frac{1}{2}\mu_0\bar{\mu}B^2\right) - \frac{(\varphi_x - \varphi_y)\rho\alpha^2\bar{\mu}}{2\varphi_y}\frac{\partial}{\partial x}\left(B\frac{\partial u}{\partial y}\right)\Big|_{y=-l}^{y=0} \quad (17)$$

Also, by using (12), one can obtain

$$\frac{\partial}{\partial x}\left(B\frac{\partial u}{\partial y}\right)\Big|_{y=-l}^{y=0} = \frac{\partial}{\partial x}\left\{\frac{Bl}{\left(1-\frac{\rho\alpha^2\bar{\mu}B}{2\eta}\right)}\frac{\partial}{\partial x}\left(p - \frac{1}{2}\mu_0\bar{\mu}B^2\right)\right\} \quad (18)$$

Form (17) and (18),

$$\frac{\partial}{\partial y}\left(P - \frac{1}{2}\mu_0\bar{\mu}B^2\right)\Big|_{y=0} = -\frac{\varphi_x l}{\varphi_y}\frac{\partial^2}{\partial x^2}\left(P - \frac{1}{2}\mu_0\bar{\mu}B^2\right) - \frac{(\varphi_x - \varphi_y)\rho\alpha^2\bar{\mu}}{2\varphi_y}\frac{\partial}{\partial x}\left\{\frac{Bl}{\eta\left(1-\frac{\rho\alpha^2\bar{\mu}B}{2\eta}\right)}\frac{\partial}{\partial x}\left(p - \frac{1}{2}\mu_0\bar{\mu}B^2\right)\right\} \quad (19)$$

Since the components of fluid velocity are continuous across the surface $y = 0$, $w|_{y=0} = \dot{h} - \bar{w}|_{y=0}$. Hence from (14),

$$w|_{y=0} = \dot{h} + \frac{\varphi_y}{\eta}\frac{\partial}{\partial y}\left(P - \frac{1}{2}\mu_0\bar{\mu}B^2\right)\Big|_{y=0} - \frac{\varphi_y\rho\alpha^2\bar{\mu}}{2\eta}\frac{\partial}{\partial x}\left(\frac{-sh^2B}{2\eta(1+hs)\left(1-\frac{\rho\alpha^2\bar{\mu}B}{2\eta}\right)}\frac{\partial}{\partial x}\left(p - \frac{1}{2}\mu_0\bar{\mu}B^2\right)\right) \quad (20)$$

Now the equation of continuity in the film (non-porous) region is

$$\frac{\partial u}{\partial x} + \frac{\partial w}{\partial y} = 0. \quad (21)$$

Putting the value of u from (12) and integrating the resultant equation with respect to y one gets

$$\frac{\left[\frac{y^3}{3}(hs+1) - \frac{h^2y^2s}{2} - h^2y\right]_{y=0}^{y=h}}{2\eta(1+hs)\left(1-\frac{\rho\alpha^2\bar{\mu}B}{2\eta}\right)^2}\left[\left(1 - \frac{\rho\alpha^2\bar{\mu}B}{2\eta}\right)\frac{\partial^2}{\partial x^2}\left(P - \frac{1}{2}\mu_0\bar{\mu}B^2\right) + \frac{\rho\alpha^2\bar{\mu}}{2\eta}\frac{\partial B}{\partial x}\frac{\partial}{\partial x}\left(P - \frac{1}{2}\mu_0\bar{\mu}B^2\right)\right] + w_h - w_0 = 0 \quad (22)$$

Using (19) and (16) in (22) yields

$$\frac{\partial}{\partial x}\left[\left\{-12\varphi_x l + \frac{(4+hs)h^3 + \left(3s\rho\alpha^2\bar{\mu}\varphi_y h^2B/\eta\right)}{(1+hs)\left(1-\frac{\rho\alpha^2\bar{\mu}H}{2\eta}\right)} - \frac{6\rho\alpha^2\bar{\mu}(\varphi_x - \varphi_y)lB}{\eta\left(1-\frac{\rho\alpha^2\bar{\mu}B}{2\eta}\right)}\right\}\frac{\partial}{\partial x}\left(p - \frac{1}{2}\mu_0\bar{\mu}B^2\right)\right] = -12\eta\dot{h} \quad (23)$$

Presenting the non-dimensional quantities

$$X = \frac{x}{L}, \quad \bar{h} = \frac{h}{h_2}, a = \frac{h_1}{h_2}, \quad \bar{p} = \frac{-{h_2}^3 p}{\eta\dot{h}L^2}, \quad \mu^* = \frac{-K\mu_0\bar{\mu}{h_2}^3}{\eta\dot{h}}, \quad \overline{L_1} = \frac{L_1}{L}, \bar{s} = sh_2,$$

$$\psi_x = -\frac{\varphi_x l}{{h_2}^3}, \quad \beta = \frac{\rho\alpha^2\bar{\mu}\sqrt{K}L}{2\eta}, \quad \gamma^* = \frac{6\varphi_y}{{h_2}^2}, \quad \psi_y = \frac{\varphi_y l}{{h_2}^3}$$

and $B^2 = Kx(L - x)$gives $B = L\sqrt{K}\sqrt{X(1-X)}$, (23) reduces to the Reynold's type equation

$$\frac{d}{dX}\left[G\frac{d}{dX}\left(\bar{p} - \frac{\mu^* X(1-X)}{2}\right)\right] = 12, \quad (24)$$

where

$$G = 12\psi_x + \frac{\bar{h}^3(4+\bar{h}\bar{s}) + \bar{s}\beta\gamma^*\bar{h}^2\sqrt{X(1-X)}}{(1+\bar{h}\bar{s})\left(1-\beta\sqrt{X(1-X)}\right)} + \frac{12\beta(\psi_x + \psi_y)}{1-\beta\sqrt{X(1-X)}} \quad (25)$$

5. Solution

For the first step$(0 \le x \le L_1)$

The non-dimensional pressure $\bar{p} = \overline{p_1}$ in the first step is obtained by taking $\bar{h} = a$ in (24) and solving under pressure boundary conditions $\bar{p} = \overline{p_1} = 0$ at $X = 0$ and $\bar{p} = \overline{p_c}$ (here $\overline{p_c}$ is non-dimensional pressure at step) at $X = \overline{L_1}$. Hence

$$\overline{p_1} = \frac{\mu^* X(1-X)}{2} + \int_0^X \left\{ \frac{12X + \frac{1}{I_1}\left\{\overline{p_c} - \frac{\mu^* \overline{L_1}(1-\overline{L_1})}{2} - 12I_4\right\}}{G} \right\} dX, \tag{26}$$

where $I_1 = \int_0^{\overline{L_1}} \frac{1}{G} dX$, $I_4 = \int_0^{\overline{L_1}} \frac{X}{G} dX$.

For the second step$(L_1 \le x \le L)$

The non-dimensional pressure $\bar{p} = \overline{p_2}$ in the second step is obtained by taking $\bar{h} = 1$ in (24) and solving under pressure boundary conditions $\bar{p} = \overline{p_2} = 0$ at $X = 1$ and $\bar{p} = \overline{p_c}$ at $X = \overline{L_1}$. Thus

$$\overline{p_2} = \frac{\mu^* X(1-X)}{2} + 12\left(\int_0^X \frac{X}{G} dX - I_2\right) + \left(\frac{\left(\int_0^{X_1} \frac{}{G} dX - I_2\right)}{(I_1 - I_2)} \left\{ \overline{p_c} - \frac{\mu^* \overline{L_1}(1-\overline{L_1})}{2} - 12I_4 + 12I_3 \right\} \right), \tag{27}$$

where $I_2 = \int_0^1 \frac{1}{G} dX$, $I_3 = \int_0^1 \frac{X}{G} dX$.

Since the flow rate at $x = L_1$ is continuous,

$$-\frac{{h_1}^3}{12\eta}\frac{dp_1}{dx} = -\frac{{h_2}^3}{12\eta}\frac{dp_2}{dx}$$

which in non-dimensional form becomes

$$a^3 \frac{d\overline{p_1}}{dX} = \frac{d\overline{p_2}}{dX} \text{ at } X = \overline{L_1} \tag{28}$$

The pressure at $x = L_1$ is $\overline{p_c}$ which can be obtained from (26), (27) and (28) as

$$\overline{p_c} = \frac{1}{\left(\frac{a^3}{G}\frac{1}{I_1} - \frac{1}{G(I_1 - I_2)}\right)} \left[\frac{1}{2}\mu^*(1-2X)(1-a^3) + \frac{1}{G}\left\{ \frac{a^3}{I_1}\left\{ \frac{1}{2}\mu^* \overline{L_1}(1-\overline{L_1}) + 12I_4 \right\} + \frac{1}{I_1 - I_2}\left\{ -\frac{1}{2}\mu^* \overline{L_1}(1-\overline{L_1}) - 12I_4 + 12I_3 \right\} \right\} \right] \tag{29}$$

The non-dimensional load capacity obtained as

$$\bar{w} = \left(\frac{\mu^*}{12}\left(3\overline{L_1}^2 - 2\overline{L_1}^3\right) + \int_0^{\overline{L_1}} \frac{1}{G}\left[12X + \frac{1}{I_1}\left\{ \overline{p_c} - \frac{\mu^* \overline{L_1}(1-\overline{L_1})}{2} - 12I_4 \right\}(\overline{L_1} - X) \right] dX \right) + \left(\frac{\mu^*}{12}\left(1 - 3\overline{L_1}^2 + 2\overline{L_1}^3\right) + 12\int_0^{\overline{L_1}} (1-\overline{L_1})\frac{X}{G} dX + 12I_5 - 12(1-\overline{L_1})I_3 + \{I_6 + I_7 - (1-\overline{L_1})I_2 I^*\} \right) \tag{30}$$

where $I_5 = \int_{L_1}^1 (1-X)\frac{X}{G} dX$, $I_6 = \int_0^{\overline{L_1}} (1-\overline{L_1})\frac{1}{G} I^* dX$, $I_7 = \int_{L_1}^1 (1-X)\frac{1}{G} I^* dX$, $I^* = \frac{1}{(I_1 - I_2)}\left\{ \overline{p_c} - \frac{\mu^* \overline{L_1}(1-\overline{L_1})}{2} - 12I_4 + 12I_3 \right\}$ and

$$\bar{w} = \int_0^{\overline{L_1}} \overline{p_1} dX + \int_{\overline{L_1}}^1 \overline{p_2} dX.$$

6. Results and Discussions

Using Simpson's one-third Rule with $n = 10$ and for water-based magnetic fluid having density $\rho = 1400\ kg/m^3$ and viscosity $\eta = 0.012\ kg/ms$ and for fixed values of $h_1 = 0.00025\ m$, $h_2 = 0.00013\ m$, $\bar{\mu} = 0.05$, $\alpha^2 = 0.0001, \alpha = 6.06$, $\dot{h} = -0.05\ m/s$, $\varphi_x = 10^{-9}$, $\varphi_y = 10^{-10}$, $L\ (= L_1 + L_2) = 0.02\ m$, the results for non-dimensional load carrying capacity (using eq.(29)) are computed based on various tables.

Moreover, when $K = 0$; FF effect without magnetic field and $K \neq 0$, FF effect with the applied magnetic field. Similarly, $\alpha^2 = 0$; represents NR model and $\alpha^2 = 0.0001$ represents the Jenkins model.

The calculation of magnetic field strength is shown below:

From equation (11)

$$B^2 = Kx(L - x),$$

$$Max\ B^2 = 10^{-4}K$$

For an example, $B = O(10^6),\ K = O(10^{16})$

Table 1 $\bar{w}$ for various values of K and step size L_1 using NR Model

$L_1 \rightarrow$ / $K \downarrow$	0.01	0.012	0.014	0.016	0.018
0	16.658	15.309	13.6784	13.8694	16.1896
$\mathbf{10^{15}}$	16.682	15.3336	13.7044	13.8992	16.2315
$\mathbf{10^{16}}$	16.893	15.5548	13.9383	14.1682	16.6082
$\mathbf{10^{17}}$	19.002	17.7661	16.2779	16.8574	20.3755
$\mathbf{10^{18}}$	40.094	39.8795	39.6731	43.7495	58.0484

Table 2 $\bar{w}$ for various values of K and step size L_1 using JE Model

$L_1 \rightarrow$ / $K \downarrow$	0.01	0.012	0.014	0.016	0.018
0	16.6582	15.309	13.6784	13.8694	16.1896
$\mathbf{10^{15}}$	14.903	17.0781	23.2918	33.7996	65.5345
$\mathbf{10^{16}}$	15.1898	17.335	23.5442	34.087	65.9755
$\mathbf{10^{17}}$	18.0607	19.9052	26.0667	36.9591	70.3853
$\mathbf{10^{18}}$	46.7708	45.6081	51.2923	65.6789	114.4824

From Table-1 and Table-2, the better $\bar{w}$ obtained when considering Ferro-fluid as a lubricant compared to conventional fluid with applied magnetic field effect. It is clear from Table-1 and Table-2, in the case of both the Models, variation in $\bar{w}$ observed when K starts with 10^{15} and sudden increase in $\bar{w}$ seen when $K = 10^{17}$ or more. From the above tabular values, better $\bar{w}$ is observed in JE Model as compared to NR Model.

Also, Table-1 shows that considering NR Model, step size directly affects values of $\bar{w}$ in the presence of Ferro-fluid as a lubricant under applied external magnetic field. However, when one considers step size 0.016 to 0.018, better $\bar{w}$ is obtained.

From Table-2, an increase in step size results in better $\bar{w}$ and drastic increase in $\bar{w}$ seen for step size 0.018. Such a scenario is not seen without a magnetic field effect.

Table 3 $\bar{w}$ for various values of φ_y and step size L_1 using NR Model for fixed $\varphi_x = 10^{-9}$

$L_1 \rightarrow$ / $\varphi_y \downarrow$	0.01	0.012	0.014	0.016	0.018
$\mathbf{10^{-7}}$	16.8926	15.5548	13.9383	14.1682	16.6082
$\mathbf{10^{-8}}$	16.8926	15.5548	13.9383	14.1682	16.6082
$\mathbf{10^{-9}}$	16.8926	15.5548	13.9383	14.1682	16.6082

From Table-3, for fixed $\varphi_x = 10^{-9}$ and considering NR Model, no change in $\bar{w}$ is observed for any value of φ_y for the same step size. Moreover, $\bar{w}$ is lowest when step size is 0.014 for any value of φ_y between 10^{-7} to 10^{-9}.

Table 4 $\bar{w}$ for various values of φ_y and step size L_1 using JE Model for fixed $\varphi_x = 10^{-9}$

$L_1 \rightarrow$ / $\varphi_y \downarrow$	0.01	0.012	0.014	0.016	0.018
$\mathbf{10^{-7}}$	6306.470	7322.698	8486.550	10302.701	13576.344
$\mathbf{10^{-8}}$	54.5328	125.0085	174.5669	196.9387	12.5083
$\mathbf{10^{-9}}$	16.8926	15.5548	13.9383	14.1682	16.6082

From Table-4, for fixed $\varphi_x = 10^{-9}$ and considering JE Model, better $\bar{w}$ is obtained when $\varphi_y = 10^{-7}$ for any step size. Also $\bar{w}$ decreases when there is a decrease in φ_y.

Table 5 $\bar{w}$ for various values of φ_x and step size L_1 using NR Model for fixed $\varphi_y = 10^{-10}$

$L_1 \rightarrow$ / $\varphi_x \downarrow$	0.01	0.012	0.014	0.016	0.018
10^{-7}	832.080	1545.557	2120.402	2637.070	2804.435
10^{-8}	46.3279	83.8343	111.5993	127.5897	66.3641
10^{-9}	16.8926	15.5548	13.9383	14.1682	16.6082

From Table-5, for fixed $\varphi_y = 10^{-10}$ and considering NR Model, better $\bar{w}$ is obtained when $\varphi_x = 10^{-7}$ for any step size. Also $\bar{w}$ decreases when there is decrease in φ_y.

Table 6 $\bar{w}$ for various values of φ_x and step size L_1 using JE Model for fixed $\varphi_y = 10^{-10}$

$L_1 \rightarrow$ / $\varphi_x \downarrow$	0.01	0.012	0.014	0.016	0.018
10^{-7}	2985.401	2252.034	2008.338	2461.108	5983.954
10^{-8}	77.6486	32.3702	8.6277	12.9484	183.7435
10^{-9}	15.1898	17.3350	23.5442	34.0870	65.9755

From Table-6, for fixed $\varphi_y = 10^{-10}$ and considering JE Model, better $\bar{w}$ is obtained when $\varphi_x = 10^{-7}$ for any step size. Also $\bar{w}$ decreases when there is a decrease in φ_y.

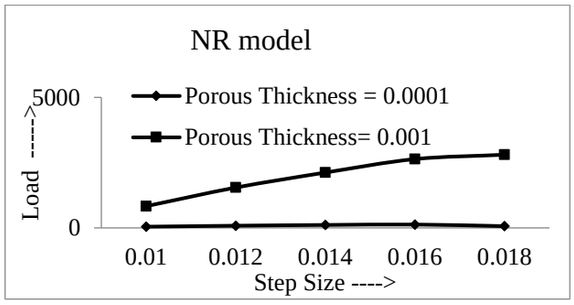

Fig. 2 $\bar{w}$ for various step size and porous thickness 0.0001 *m* and 0.001 *m* (NR Model)

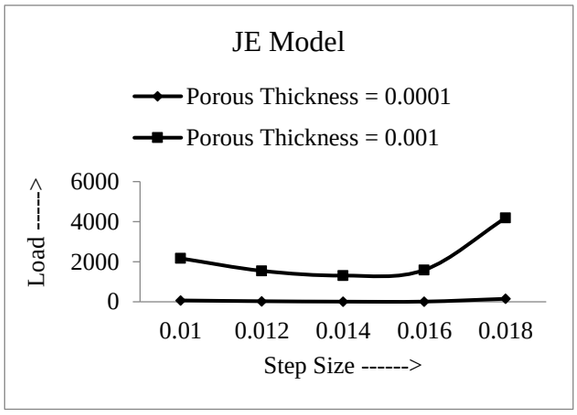

Fig. 3 $\bar{w}$ for various step sizes and porous thickness 0.0001 *m* and 0.001 *m* (JE Model)

From Figure-2 and Figure-3, it is seen that better $\bar{w}$ is obtained when the uniform thickness of the attached porous layer is 0.001 *m* in both the models, and hence the concept of self-lubrication is fulfilled. Also, from Figure-2, $\bar{w}$ regularly increases with the increase of first step size. But this kind of scenario is not seen in JE Model. That means $\bar{w}$ decreases up to approximately the first step size up to 0.015 and then suddenly increases.

7. Conclusions

This study concludes that to design a Porous Step Bearing by considering NR Model or JE Model; the following points should be considered:

- One should prefer ferrofluid as lubricant over conventional fluid under applied magnetic field effect for a better load.
- Preferably, one should choose a step size from 0.016 to 0.018.
- The thickness of the assorted porous layer should be minimal.
- φ_y doesn't play any role when one considers NR Model with $\varphi_x = 10^{-9}$ and other suggested parameters.
- Preferable values of φ_x is $10^{-9}$and φ_y is 10^{-7} if one prefers JE Model.
- It is better to consider JE Model over NR Model to design such a bearing.

References

1. *Leek TH, Lingard S, Atkin RJ, et al. (1993), An experimental investigation of the flow of an electro-rheological fluid in a Rayleigh step bearing. J. Phys. D; Vol. 26: 1592–1600.*
2. *Shah RC (2003), Ferrofluid lubrication in step bearing with two steps, Ind. Lubric. Tribol., Vol. 55(6): 265–267.*
3. *Shah RC and Patel N I (2014), Impact of various and arbitrary porous structure in the study of squeeze step bearing lubricated with magnetic fluid considering variable magnetic field, Proc IMechE Part J: J Engineering Tribology, Vol. 229(5): 646-659.*
4. *Rosensweig RE (1985), Ferrohydrodynamics. New York: Cambridge University Press.*
5. *Shah RC and Bhat MV (2000), Squeeze film based on magnetic fluid in curved porous rotating circular plates, J Magnet Magnet Mater, Vol. 208: 115–119.*
6. *Bashtovoi VG and Berkovskii BM (1973), Thermomechanics of ferromagnetic fluids. MagnitnayaGidrodinamika, Vol. 3: 3–14.*
7. *Goldowsky M. (1980), New methods for sealing, filtering, and lubricating with magnetic fluids, IEEE Trans Magnet, Vol. 16: 382–386.*
8. *Popa NC, Potencz I, Brostean L, et al. (1997), Some applications of inductive transducers with magnetic fluids. Sens Actuat A, Vol. 59: 197–200.*
9. *Liu J. (2009), Analysis of a porous elastic sheet damper with a magnetic fluid, J Tribol., Vol. 131: 0218011–15.*
10. *Verma PDS. (1986), Magnetic fluid-based squeeze film, Int J Eng Sci, Vol. 24(3): 395–401.*
11. *Shah RC and Patel DB. (2012), Mathematical modeling of newly designed ferrofluid based slider bearing includingeffects of porosity, anisotropic permeability, slip velocityat both the ends, and squeeze velocity, Appl Math, Vol. 2(5): 176–183.*
12. *Sparrow EM, Beavers GS and Huang IT. (1972), Effect of velocity slip on porous walled squeeze films, J Lubric Technol Vo. 94: 260–265.*
13. *Patel DA, Attri MJ, Patel DB. (2021), Performance of Hydrodynamic Porous Slider Bearing with Water based Magnetic Fluid as a Lubricant: Effect of Slip and Squeeze Velocity, Journal of Scientific & Industrial Research, Vol. 80: 508-512.*
14. *Bhat MV. (2003) Lubrication with a Magnetic Fluid, Team Spirit India, Ahmedabad, India.*
15. *Jenkins JT. (1972), A theory of magnetic fluids, Archive for Rational Mechanics and Analysis, Vol. 46: 42–60.*
16. *Ram P. and Verma PDS. (1999), Ferrofluid lubrication in porous inclined slider bearing, Indian Journal of Pure and Applied Mathematics, Vol. 30(12): 1273–1281.*
17. *Prakash J. and Vij SK. (1973), Hydrodynamic lubrication of a porous slider, J. Mech, Engg. Sci., Vol. 15: 232–234.*